Fabry-Perot Diaphragm Fiber Optic Sensor (DFOS) for Acoustic Detection

Y. Sun*, G. Feng*, G. Georgiou*, I. Padron*, N. Edip*, K. Noe** and K. Chin*

*New Jersey Institute of Technology, Materials Science Program, 07031 USA, ys2@njit.edu
**PSE&G Corporation, Newark, NJ, USA, Karen.Noe@pseg.com

ABSTRACT

The diaphragm fiber optic sensor (DFOS) solely based on Fabry-Perot multiple beam interference has been designed and fabricated with Micro-electric mechanical system (MEMS) technology. The silicon diaphragm with an embossed center was designed with an interference gap width kept accurately. The DFOS is verified to be truly and purely of Fabry-Perot type via a critical test. Parallel testing of DFOS in comparison with a Piezoelectric (PZT) sensor shows that DFOS has high sensitivity. Fabry-Perot DFOS has demonstrated excellent performances in on-line monitoring of Partial Discharge (PD) in power transformers.

Keywords: MEMS, Fabry-Perot, fiber optic, acoustic, diaphragm with embossed center

1 INTRODUCTION

A diaphragm fiber optic sensor (DFOS) utilizes a diaphragm as the sensing element to detect static and dynamic pressure (acoustic wave). The fiber is used to deliver a steady probing light and to receive the reflected light modulated by the signals under detection. In recent years diaphragm-based fiber optic sensors have been developed for static pressure and acoustic signal detection due to its high sensitivity, flexibility, and versatility of its diaphragm-fiber structure, as well as resistance to electromagnetic interference (EMI) caused noise, and easiness for multiplexing and integration [1-4]. In this research, the silicon diaphragm was designed to have an embossed center and micro-channels in order to improve efficiency, alignment, linearity, and Q-point stability which are still critical issues in diaphragm-based fiber optic sensor design.

Currently an imminent application of DFOS is detecting partial discharge (PD) in high voltage transformers in the power industry. PD is an electrical discharge that occurs in an insulation system where the charge does not completely bridge the electrodes. It is a well-known phenomenon and a precursor to complete insulation failure. Partial discharge within the power transformer could lead to degradation of the insulation system and may therefore result in catastrophic failures [5-9]. It is a big concern for the power industry. As a consequence, there is a strong need for a capable sensor to detect and study PD.

2 SENSOR SYSTEM DESIGN

2.1 Sensor System Configuration

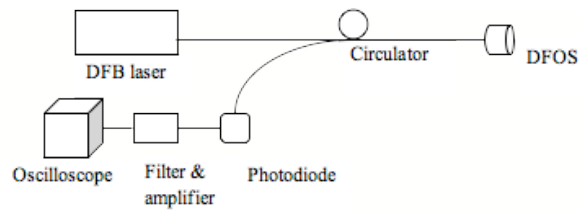

Figure 1: Schematic of DFOS system.

The acoustic detection system is illustrated schematically in Figure 1. Acoustic signal is detected by using the developed DFOS system, which consists of a DFOS, a 1527 nm DFB laser, a 3-port fiber circulator, a photodiode and a filter and amplification circuit. The light from DFB laser propagates along the single mode fiber to the DFOS through the circulator and interferes inside the DFOS. The modulated light propagates back in the third leg of the circulator and is detected by the photodiode. The optical signal is turned into electric signal. Its output voltage is filtered and amplified and finally processed and collected by an oscilloscope.

2.2 Sensor Operation Principle

Fabry-Perot interferometric device is based on the interference of multiply reflected beams. The interference gap L corresponding to applied pressure is determined by measuring the inference spectrum. The spectrum of the ratio of output and input optical power is defined as.

$$\frac{I^{(0)}}{I^{(i)}} = \frac{2R_a - 2R_g \cos\phi}{1 + R_g^{\,2} - 2R_g \cos\phi} \qquad (1)$$

where R_a is the arithmetic mean reflectance of the interfaces, R_g is the geometric mean reflectance of the interfaces, and ϕ is the phase shift of the light propagating across the interference gap L.

The mechanism of DFOS is usually described by the Fabry-Perot interference of multiply reflected beams between the diaphragm surface and the fiber end surface. The structure of the Diaphragm Fiber Optic Sensor (DFOS) is shown in Figure 2. The diaphragm, as the sensing

element, is batch fabricated on a silicon wafer with MEMS technology and is bonded to single mode optic fiber utilizing soldering to keep the sensor cavity at Q-point. Fabry Perot interferemetry is formed between the fiber end face and diaphragm inner surface. The incident light is partially reflected at the end face of the fiber. The remainder of the light crosses through the air gap, partially reflected at the inner surface of the diaphragm and finally transmitted back to the fiber. The acoustic pressure changes the air gap and modulates the light transmitted back through the fiber. Sensitivity, efficiency and frequency response, etc. are determined by the geometry of the diaphragm. Therefore diaphragm design is critical part of the sensor construction.

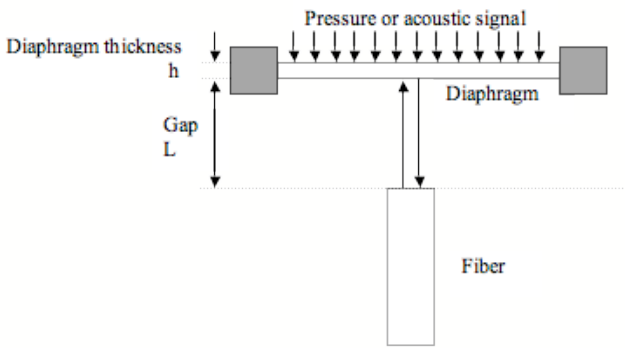

Figure 2: Principle of Diaphragm Fiber Optic Sensor(DFOS).

2.3 Diaphragm Design Consideration

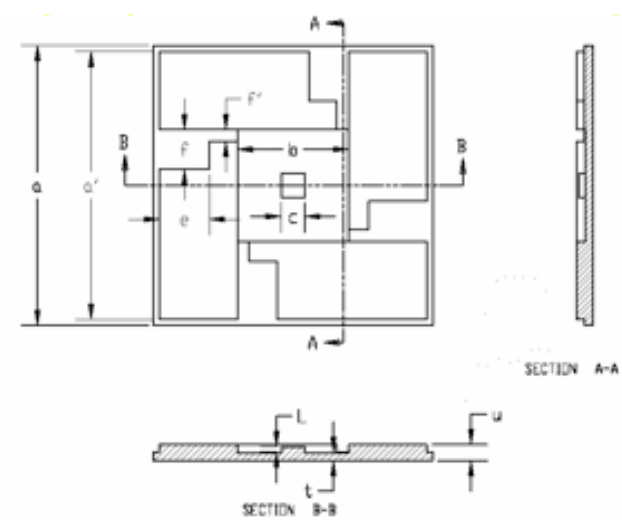

Figure 3: Schematic diagram of Silicon diaphragm with embossed center and micro-channels.

The thickness and side length of the diaphragm are selected depended on the pressure range and acoustic frequency that the device is required to operate. The center deflection y_0 (m) of a flat square diaphragm under pressure may expressed by the equation[10,11]:

$$y_0 = \alpha \frac{Pa^4(1-v^2)}{Eh^3} \tag{2}$$

where a is half side length of the square diaphragm, h is the thickness, P is applied pressure, E is Young's modulus and ν is Poisson ratio.

For the diaphragms clamped at its circumference, the resonant frequency is

$$f = \frac{\pi}{a^2} \cdot \left[\frac{gD}{hw} \right]^{\frac{1}{2}} \tag{3}$$

where D is flexural rigidity, w is the diaphragm density .

Embossed center was designed in the diaphragm of DFOS to make the structure stable. The distance between diaphragm and end face of the fiber must keep within several micrometers for near field operation. One of advantages of the embossed center is it can avoid the lateral misalignment. The other important advantage of the embossed center in the diaphragm design is it reduces considerably the back pressure in the air cavity, which will reduce the sensibility of the DFOS.

For the sensors using in large temperature range, the thermal drift is caused by expansion of the air in the sensor cavity, and gap width will be off the Q-point. Four micro-channels were design in order to compensate the air expansion.

A smaller interference gap not only void potential misalignment caused loss and noise, but also increases the efficiency. The air-gap of DFOS is 2 μm so the diaphragm was designed very close to the fiber end, and the reflection intensity increased dramatically. According to mirror symmetry of the electromagnetic wave, the coupling coefficient of the electromagnetic wave back into the fiber is decrease proportional to the beam spreading through a air gap distance and how may times the light was reflected.

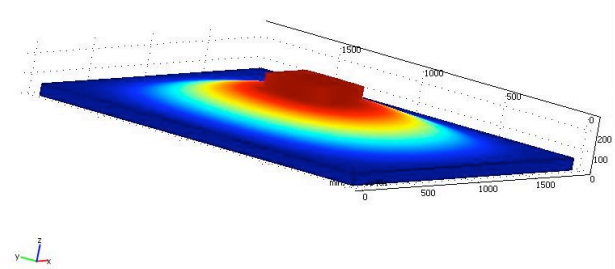

Figure 4: 3D Femlab simulation of the diaphragm with embossed center.

Femlab was used for simulation in resonant frequency and center deflection of diaphragm with embossed center (Figure 4). For PD acoustic detection, the diaphragm with 1.9mm side length, 60 μm thickness and 2 μm interference gap was selected.

3 SENSOR FABRICATION

The diaphragm procedure using MEMS technology is shown in Figure 5. A 220 µm Silicon wafer was etched to 60 µm on both sides in KOH. The embossed center was protected. Thus, the Silicon surface of the diaphragm was remaining intact. Both surfaces in the Fabry-Perot cavity, the diaphragm embossed center and fiber end, are perfect flat surfaces to reducing speckle noise. The surrounding wall at font side of the diaphragm was coated with gold by evaporation. The gap is accurately determined by the Gold film thickness.

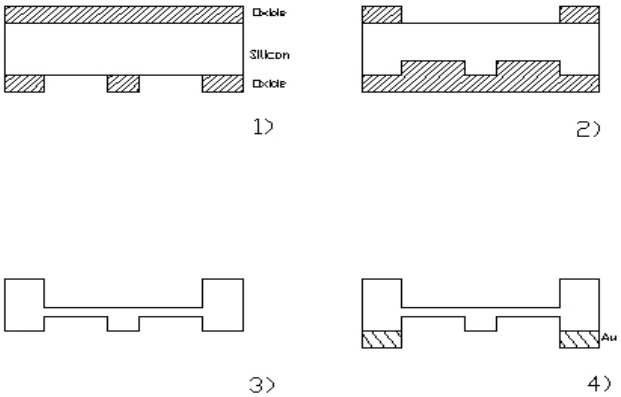

Figure 5: Schematic of process for diaphragm.

The diaphragm and fiber tip was mechanical clamped. Alignment and Q-point was adjustable by controlling the reflective light power for linear operation and the highest detection sensitivity. After confirming that the reflection light of the sensor is reached Q-point, the surrounding of the diaphragm is soldered by Ag-Sn-Pb175 under microscope with the fiber ferule.

4 EXPERIMENTAL RESULTS

4.1 Static Pressure Test

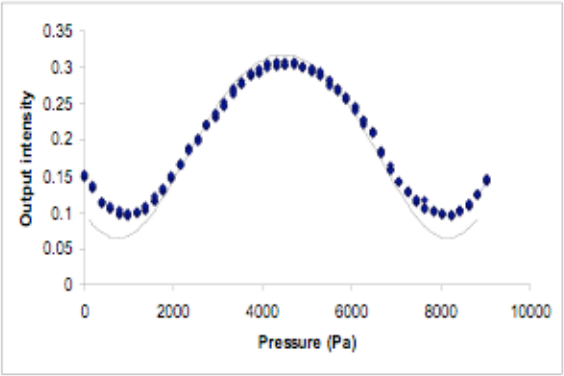

Figure 6: Static characterization of optic output (dotted line) as a function of pressure, in comparison with calculated curve from Equation (1)

Static pressure testing was firstly demonstrated in Diaphragm based Fabry-Perot sensors. Static pressure is measured up to 35 psi which is equal to 16 meter water height. The intensity vs. pressure curve is shown in Figure 6. The good agreement of he theoretical curve calculated from Equation (1) and experimental data was achieved. Therefore, DFOS has been proved as truly and purely Fabry-Perot devices.

A DFOS and a PZT sensor were tested in parallel under identical conditions. DFOS and R15 (a commercial PZT sensor made in Physics Acoustic Corporation) were immersed into water. The Acoustic waves were created by an emitter (pulser R15) placed approximately 8 inches away from both sensors. The pre-amp gain of R15 sensor was set to 20 dB. DFOS is connected directly to the oscilloscope without any amplification system.

Figure 7 (a) and (b) show the waveforms and frequency spectra of DFOS and R15 when the pulser frequency was 130 kHz. Both sensor types exhibit very similar waveform profiles and frequency spectra.

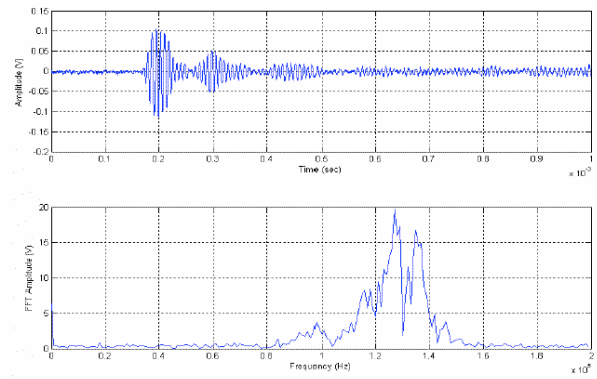

(a)

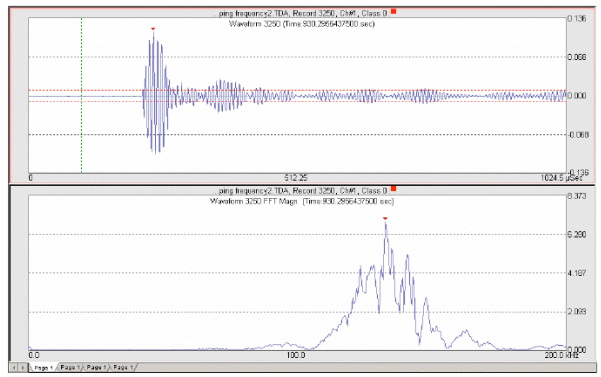

(b)

Figure 7: Waveform and frequency spectrum when the pulser frequency is 130kHz. (a) DFOS (b) PZT sensor.

The pulser frequency was increased with 5 kHz increments, from 75 kHz to 300kHz. In Figure 8, the acoustic pressure response spectrum of DFOS and PZT is shown. R15 sensor with 20 dB gain has two bandwidths with peak frequencies at 150 kHz and 230 kHz. The maximum amplitude is about 145 and 185 mV respectively. DFOS without amplification have a bandwidth with a peak frequency about 105 kHz. The maximum amplitude of

DFOS is about 140 mV and DFOS has shown high sensitivity.

4.2 Partial Discharge Acoustic Detection

The DFOS is put in the oil of a retired real utility transformer at different position to the spark. The PZT sensor is attach to the tank wall for external PD detection.

In Figure 9, the purple curves of extremely high frequency are the triggering signal of the PD. It is served as the starting time of the occurrence of the PD. The time difference from the end of the purple electrical signal to the onset of the yellow acoustic signal is the time of flight. It clearly shows the time of flight is increased as the sensor moving away from the spark.

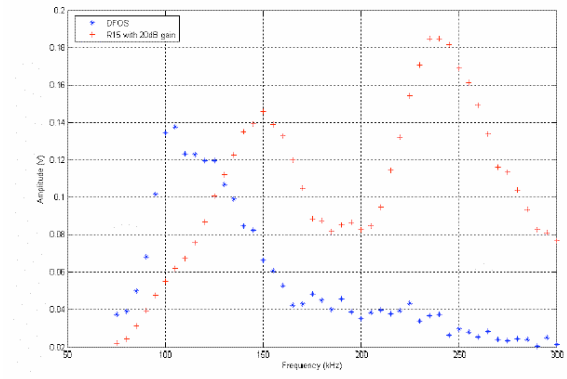

Figure 8: Amplitude distribution of DFOS and R15 with respect to frequency.

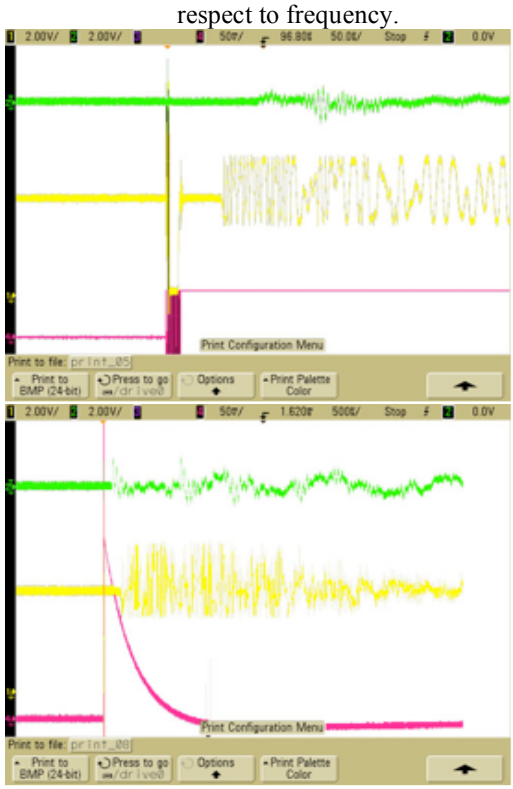

Figure 9: PD in the oil tank of a transformer detected by DFOS and PZT sensor.

5 CONCLUSION

The Diaphragm fiber Optic Sensor is based on extrinsic Fabry-Perot interferemetry. A designed diaphragm is the sensing element of the sensor. Bonding method and diaphragm processing make the diaphragm and fiber both laterally and angularly aligned. It made the sensor to achieve better alignment and Q-point stabilized, thus, DFOS is more reliable and with high efficiency. Static pressure and dynamic acoustic measurements are highly desirable to improve its operation and reliability. High frequency (100kHz) DFOS has shown high sensitivity when it was tested in comparison with commercial PZT sensors.

REFERENCES

[1] Totsu K., Haga, Y. and Esashi, M. "Ultra-Miniature Fiber-Optic Pressure Sensor Using White Light Interferemtry." Journal of Micromechanics and Microengineering Vol.15, 71-75, 2004.

[2] Yu, M. and Balachandran, B. "Sensor Diaphragm Under Initial Tension: Linear Analysis." Society for Experimental Mechanics. 123-127, 2005

[3] Zhu, Y., and Wang, A. "Miniature Fiber-Optic Pressure Sensor." IEEE Photonic Technology Letters, Vol.17, No. 2, 447-449. 2005.

[4] Xu, J., Wang, X., Cooper, K. and Wang, A. "Miniature All-Silica Fiber Optic Pressure and coustic Sensor." Optic Letters. Vol.30, No.24, 3269-3271, 2005.

[5] Bartnikas, R. "Partial Discharges Their Mechanism, Detection and Measurement." IEEE Transactions on Dielectrics and Electrical Insulation, Vol. 9, No. 5. 763, 2002.

[6] Harrold, R. "Partial Discharge – Part XVI: Ultrasonic Sensing of PD within Large Capacitors. "IEEE Electrical Insulation Magazine, Vol. 9, No.3, 1993.

[7] Lundgaard, L.E. Partial Discharge – Part XIII: Acoustic Partial Discharge Detection – Fundamental Considerations. IEEE Electrical Insulation Magazine, Vol.8, No.4, 1992.

[8] Lundgaard, L. "Partial Discharge – Part XIV: Acoustic Partial Discharge Detection – Practical Application." IEEE Electrical Insulation Magazine, Vol. 8, No. 5, 1992

[9] Eleftherion, P. "Partial Discharge XXI: Acoustic Emission-Based PD Source Location in Transformers." IEEE Electrical Insulation Magazine, Vol. 11, No. 6, 1995.

[10]Timoshenko and Woinowski-Krieger, "Theory of Plates and Shells," McGraw-Hill,1959.

[11]Giovanni, M.D. "Flat and Corrugated Membrane Design Handbook". Mercel Dekker Inc., New York.